

Cracking in Connections Between Floorbeams
and Supporting Girders - Development and
Use of a Portable Strain Monitoring
System for Bridge Evaluations

Richard R. Sartor
Graduate Assistant

John T. DeWolf
Professor

March 1, 1996

JHR 96-246

Final Report

Project 92-2

This research was sponsored by the Joint Highway Research Advisory Council (JHRAC) of the University of Connecticut and the Connecticut Department of transportation and was carried out in the Civil and Environmental Engineering Department of the University of Connecticut.

The contents of this report reflect the view of the author (s) who are responsible for the facts and accuracy of the data presented herein. The contents do not necessarily reflect the official views or policies of the University of Connecticut or the Connecticut Department of Transportation. This report does not constitute a standard, specifications, or regulations.

1. Report No. JHR 96-246		2. Government Accession No.		3. Recipient's Catalog No.	
4. Title and Subtitle Cracking in Connections Between Floorbeams and Supporting Girders - Development and Use of a Portable Strain Monitoring System for Bridge Evaluations				5. Report Date December 1995	
				6. Performing Organization Code	
				9. Performing Organization Report No. JHR 96-246	
7. Author(s) John T. DeWolf and Richard R. Sartor				10. Work Unit No. (TRIS)	
9. Performing Organization Name and Address University of Connecticut Department of Civil Engineering 191 Auditorium Road, Box U-37 TI Storrs, CT 06269				11. Contract or Grant No.	
				13. Type of Report and Period Covered Final Report	
12. Sponsoring Agency Name and Address Connecticut Department of Transportation 280 West Street Rocky Hill, CT 06067-0207				14. Sponsoring Agency Code	
15. Supplementary Notes					
16. Abstract This report demonstrates how field monitoring has been used to assist in the management of the State of Connecticut's bridge infrastructure. The portable strain monitoring system and software developed at the University of Connecticut are described. Four different cases studies are included. The work demonstrates that analytical predictions of stress/strain levels, load distributions and fatigue estimations are often only approximate. Field testing, combined with a careful analysis, can provide answers where analyses are approximate. The field monitoring reported in this study has resulted in substantial savings to the State of Connecticut.					
17. Key Words Bridge monitoring, strain monitoring, fatigue, diaphragms, load rating			18. Distribution Statement No Restrictions		
19. Security Classif. (of this report) Unclassified		20. Security Classif. (of this page) Unclassified		21. No. of Pages 48	22. Price

ACKNOWLEDGEMENTS

This report is adapted from the M.S. thesis submitted by Richard R. Sartor, Graduate Assistant (Reference 1). The work follows the investigation reported by DeWolf and Bernard (Reference 2).

The work began as a study to evaluate cracks in floor beam connections. The effectiveness of the field strain monitoring system was readily proven. The development of additional software provided expanded capabilities, with major reductions in the time needed for data evaluation. Consequently the researchers were able to use the system on different bridges with different problems. Thus, this report presents four case studies which best demonstrate the effectiveness of using the field monitoring system.

This work was supported by the Connecticut Department of Transportation. The assistance of Mr. Michael Culmo of the Connecticut Department of Transportation Bridge Design Unit is especially appreciated.

SI* (MODERN METRIC) CONVERSION FACTORS

APPROXIMATE CONVERSIONS TO SI UNITS				APPROXIMATE CONVERSIONS TO SI UNITS			
Symbol	When You Know	Multiply By	To Find	Symbol	When You Know	Multiply By	To Find
<u>LENGTH</u>				<u>LENGTH</u>			
in	inches	25.4	millimetres	mm	millimetres	0.039	inches
ft	feet	0.305	metres	m	metres	3.28	feet
yd	yards	0.914	metres	m	metres	1.09	yards
mi	miles	1.61	kilometres	km	kilometres	0.621	miles
<u>AREA</u>				<u>AREA</u>			
in ²	square inches	645.2	millimetres squared	mm ²	millimetres squared	0.0016	square inches
ft ²	square feet	0.093	metres squared	m ²	metres squared	10.764	square feet
yd ²	square yards	0.836	metres squared	m ²	hectares	2.47	acres
ac	acres	0.405	hectares	ha	kilometres squared	0.386	square miles
mi ²	square miles	2.59	kilometres squared	km ²			
<u>VOLUME</u>				<u>VOLUME</u>			
fl oz	fluid ounces	29.57	millilitres	mL	millilitres	0.034	fluid ounces
gal	gallons	3.785	Litres	L	litres	0.264	gallons
ft ³	cubic feet	0.028	metres cubed	m ³	metres cubed	35.315	cubic feet
yd ³	cubic yards	0.765	metres cubed	m ³			
<u>MASS</u>				<u>MASS</u>			
oz	ounces	28.35	grams	g	grams	0.035	ounces
lb	pounds	0.454	kilograms	kg	kilograms	2.205	pounds
T	short tons (2000 lb)	0.907	megagrams	Mg	megagrams	1.102	short tons (2000 lb)
<u>TEMPERATURE (exact)</u>				<u>TEMPERATURE (exact)</u>			
°F	Fahrenheit temperature	5(F-32)/9	Celcius temperature	°C	Celcius temperature	1.8C + 32	Fahrenheit temperature

NOTE: Volumes greater than 1000 L shall be shown in m³.

*SI is the symbol for the International System of Measurement

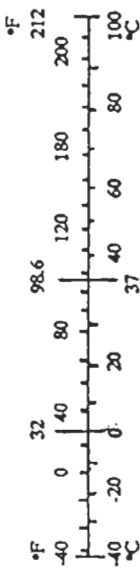


TABLE OF CONTENTS

	Page
Technical Report Documentation Page	ii
Acknowledgements	iii
Modern Metric Conversion Factors	iv
Table of Contents	v
List of Figures	vi
List of Tables	viii
Chapter 1 - Introduction	1
Chapter 2 - Strain Monitoring System	4
System Hardware	4
Effective Stress Range Software	5
Chapter 3 - Tomlinson Bridge	9
Chapter 4 - Route 7 Bridge over Still River	12
Chapter 5 - The Yankee Doodle Bridge	15
Chapter 6 - Route 8 Bridge in Trumbull	19
Chapter 7 - Conclusions	23
References	25
Figures	26
Tables	46

LIST OF FIGURES

	Page
Figure 1: Strain Gage Monitoring System	26
Figure 2: Stress Range Histogram	27
Figure 3: Tomlinson Bridge Hanger Assembly	28
Figure 4: Tomlinson Bridge - Stress VS. Time (Outside Hanger Member)	29
Figure 5: Tomlinson Bridge - Stress VS. Time (Inside Hanger Member)	30
Figure 6: Route 7 Bridge - Cracking And Strain Gage Locations	31
Figure 7: Route 7 Bridge - Typical Plot Of Stress VS. Time	32
Figure 8: Route 7 Bridge - Non-Typical Plot Of Stress VS. Time	33
Figure 9: Yankee Doodle Bridge - Plan View Of Test Span With Strain Gage Locations	34
Figure 10: Yankee Doodle Bridge - Detail With Strain Gage Location	35
Figure 11: Yankee Doodle Bridge-Typical Plot Of Stress VS. Time Gages	36
Figure 12: Yankee Doodle Bridge - Typical Plot Of Stress VS. Time	37
Figure 13: Yankee Doodle Bridge - Stress Range Histogram For Channel 0	38
Figure 14: Yankee Doodle Bridge - Stress Range Histogram For Channel 1	39
Figure 15: Yankee Doodle Bridge - Stress Range Histogram For Channel 2	40

Figure 16:	Yankee Doodle Bridge - Stress Range Histogram For Channel 3	41
Figure 17:	Route 8 Bridge - Plan View With Strain Gage Locations	42
Figure 18:	Route 8 Bridge - Detail With Strain Gage Location	43
Figure 19:	Route 8 Bridge Plot Of Stress VS. Time Data Set 06	44
Figure 20:	Route 8 Bridge Plot of Stress VS. Time	45

LIST OF TABLES

	Page
TABLE 1: Tomlinson Bridge - Maximum Stress Levels (KSI)	46
TABLE 2: Route 7 Bridge - Maximum Stresses (KSI)	47

Chapter 1

INTRODUCTION

This report demonstrates how field monitoring has been used to assist in the management of the State of Connecticut's bridge infrastructure. This study is part of a continuous effort to provide information on the performance of different bridges, both before and after renovations.

Typically, design of different parts of bridges is based on application of theory to practice, with emphasis on how the structure is presumed to behave. In even the most carefully conceived design, it is not always possible to consider all variables. Further, analytical tools are not always adequate in evaluating stresses and strains of different members and connection elements. This is particularly true with respect to localized areas in these members. Even finite element analyses, which has great potential for determining stresses and strains in specific parts, does not provide exact answers. The development of the method is based on assumptions, and any application must rely on simplifications, particularly when localized areas are

under investigation.

Areas in which field monitoring is beneficial in the evaluation of the performance include measurement of stress levels in connections, evaluation of how loads are distributed to different members, determination of deformational induced behavior and the development of fatigue predictions. Monitoring is useful to determine whether repairs are required, to assist in developing how they should be made and to evaluate the behavior following repair.

This report shows how a portable strain monitoring system has been used in the evaluation of four bridges in the State of Connecticut. The problems considered were:

- (1) Determination of stress levels in a critical hanger in an older bridge subject to corrosion.
- (2) Determination of the cause of cracking, i.e. whether it was due to fatigue loading or fabrication problems.
- (3) Determination of the effective stress range needed in

the evaluation of fatigue capacity.

(4) Determination of the live load rating in a bridge with different girder sizes.

Chapter 2

STRAIN MONITORING SYSTEM

2.1 System Hardware

Although strain monitoring is not new, recent advances in electronics have vastly improved the capabilities and data collection speed for portable acquisition hardware. The essential requirements for a portable strain gage system are the need for reliable data in a variety of test situations and the ability to collect data under normal vehicular traffic.

The basic electronics for the strain monitoring system used (MEGADAC 3008DC) was developed by Optim Electronics Corporation of Germantown, Maryland. The system was first used to study fatigue cracking (2). The system contains a memory buffer, and it is controlled by a portable computer which also allows for permanent storage of data. The full system is shown in Fig. 1.

The system software (Test Control Software) provides for different test procedures and data control. Included are user

defined data limits, which allow recording of only data in the range of interest, and triggers which allow for different lengths of data collection. These features are especially useful in determining stress histories, without collecting excessive, unneeded data. Also critical in data collection is the ability to collect and store data at sufficient speed to evaluate the dynamic component, necessary in assessing impact factors.

2.2 Effective Stress Range Software

One of the goals of this research was to automate the data analysis. Strain gage data obtained during field studies is often used to investigate fatigue cracking in steel bridges. The stress parameter governing the fatigue behavior of members is the Effective Stress Range, S_r . A program was developed to calculate the Effective Stress Range and determine the remaining fatigue life of structural members at intervals during data collection.

The Automated Effective Stress Range program calculates the Effective Stress Range S_r using the procedure described in section 2.1 (Alternative 1) of the AASHTO "Guide Specification

for Fatigue Evaluation of Existing Steel Bridges" (3). The program can also calculate the remaining fatigue life of the members, with the input of additional information by the user. This calculation follows the procedure given in Section 3 of the Guide Specification.

After defining the stress intervals the program determines the fraction of peak stress ranges falling within each interval. An example is shown in Fig. 2. This shows a graphical representation of the data in the form of a stress range histogram. The effective stress range S_r is calculated by applying Minor's rule, stated as follows:

$$S_r = (\sum f_i S_{ri}^3)^{1/3}$$

where:

f_i = Fraction of stress ranges within each interval.

S_{ri} = Stress at the midwidth of the interval.

S_r is then used to calculate the fatigue life. If the

remaining fatigue life is not infinite, the program calculates the mean and safe remaining life Y_f from the following relation:

$$Y_f = \frac{f K 10^6}{T_a C (R_s S_r)^3} - a$$

where:

- f = 1.0 for calculating safe life and 2.0 for calculating mean life.
- K = AASHTO detail constant
- T_a = Estimated lifetime average daily truck volume in the outer lane
- C = Stress cycle per truck passage
- R_s = Reliability factor
- S_r = Effective stress range
- a = Present age of bridge in years

The procedures for calculating T_a , C and R_s are presented in the guide specification.

Since the program provides a table of peak stress ranges, by

channel, for each data set recorded, it is also useful in other evaluations.

Chapter 3

TOMLINSON BRIDGE:

This study was performed to obtain stress data and assess suspected structural problems in the hangers. The age and level of corrosion made analytical assessments impossible.

The Tomlinson is located in New Haven, Connecticut, and spans the Quinnipiac River. The structure is a draw bridge consisting of two sections. Large concrete counterweights, located on the abutment sides of the main bearings, balance the superstructure weight.

Each counterweight is supported by two hangers, and each hanger consists of two I-shaped structural steel members. The counterweight hangers are connected to bearings, which allow the counterweight hangers to remain vertical for any bridge superstructure angle. The hangers are shown in Fig. 3.

The design consultant and ConnDOT personnel speculated that friction in the counterweight hanger bearings was inducing moments in addition to axial forces in the counterweight

hangers. This field test was performed to verify this assumption and determine the magnitude of the stresses. The consultant believed that the stresses in the hangers were significant and that the hangers should be strengthened immediately, even though the structure would soon be replaced.

Four strain gages were placed on both the hangers on one side of the bridge. Figure 3 shows the location of the strain gages used. Strain gage data were recorded for four complete loading cycles. A complete cycle began with the bridge at rest in the horizontal position. The bridge was then raised to the maximum vertical angle (approximately 90 degrees) and momentarily stopped. The cycle was completed by lowering the bridge to the initial (horizontal) position. The recording speed was 20 readings per second per gage.

Figures 4 and 5 present stress versus time plots for the outside and inside hanger members, respectively. The changes in stress in the gages on each hanger member during opening and closing are approximately equal in magnitude and of opposite signs. These stresses during movement thus show that the members are subject to bending. The inside member (gages 1 and 2)

experienced a maximum bending stress of 4.4 KSI. The outside member (gages 0 and 3) experienced a maximum bending stress of 6.6 KSI. The results for each recorded cycle are similar, and they are shown in Table 1.

The test results confirmed that bending occurs during opening and closing and that stress levels due to bending are significant. Calculations show that the dead load stresses are approximately equal to the allowable stresses based on the estimated section loss in the hangers. Thus it was concluded that the additional live load stresses could cause failure, resulting in a collapse. The decision was made to strengthen the hangers immediately, even though the structure would be replaced.

Chapter 4

ROUTE 7 BRIDGE OVER STILL RIVER

This study was performed to determine the cause of cracking in this steel girder bridge.

The 15 year old bridge is located in Brookfield, Connecticut. It carries CT Route 7 over Still River and Grays Bridge Road. The superstructure is a two span continuous welded plate girder bridge with a composite concrete slab deck. The five girders carry traffic in one direction only. An adjacent structure carries traffic in the other direction. Girder loads are transferred to the abutments via pot bearings. Cracks have developed in the longitudinal welds that join filler plates at the top girder flange, shown in Figure 6. The filler plates connect the bearing stiffeners to the girder flanges at the interior support. This detail was used to avoid using a direct transverse weld between the bearing stiffener and the flange.

Two strain gages were used on the first interior plate girder, located directly beneath the low speed travel lane. One

gage was placed on the upper flange and one on the lower flange near the interior support. Both were placed in the longitudinal direction. They are shown in Figure 6.

Strain gage data were recorded for 25 truck events. The test was set to record only when the stress in either flange reached +/-300PSI. This eliminated data due to small vehicle loading. The recording speed was 30 readings per second per gage.

All the data sets, except numbers 22 and 23, exhibited similar behavior. The maximum stresses are given in Table 2. Figure 7 shows a typical Stress versus Time plot for a "normal" data set. Two peaks are evident, one as the vehicle approaches the interior support and one after the vehicle passes the interior support. The magnitude and duration of the peaks are comparable. As expected, the top flange is in tension and the bottom in compression.

Plots of the stresses for Data set 23, which is not typical, are shown in Figure 8. This behavior is distinctly different from all other data sets. The top flange is in compression

(instead of tension) with a magnitude is 2.66 KSI (10 times the largest tensile reading). Also, the event duration is much shorter, with a more rapid loading rate. As the maximum stress in the top flange is reached, the stress in the bottom flange is near zero. One possibility is that the behavior is due to an eccentric axial load, rather than bending stress. This suggests that the top flange is restrained. When the restraint is released, perhaps by another vehicle, a compressive force is imparted to the deck and girder at the level of the top flange. This restraint/release behavior could be caused by constraints in the deck joints at the abutment.

The data sets show a maximum top flange tensile stress of 0.263 KSI and an average peak stress level of 0.165 KSI for live load. These stresses are well below the fatigue limit for the welds. Thus, this data suggests that these cracks are "cold cracks" which developed during fabrication, most likely because of low quality welds. They are essentially due to cooling immediately following welding. No remedial measures are therefore required.

Chapter 5

THE YANKEE DOODLE BRIDGE

This study was performed to investigate fatigue cracking in a steel bridge.

The Yankee Doodle Bridge is located in Norwalk, Connecticut. It carries Interstate 95 over the Norwalk River. The seven span superstructure has continuous welded plate girders supporting a composite concrete slab deck. There are eleven longitudinal girders. The structure is approximately 35 years old and carries a large number of trucks.

The plate girders are non-prismatic. At approximately the third points, the flange plate thickness changes from 1-1/4" to 1-3/4" in the interior girders. The plates are joined by Double-V Groove welds. Defects have been detected in many of these welds when John W. Fisher, Lehigh University, evaluated the physical characteristics of these defects (4).

Fisher and ConnDOT engineers recommended determination of

the effective stress range at the weld locations. This stress range, under representative live loading, is required to determine if the weld defects will propagate in the future. The weld defects are assumed to behave like cracks.

Four strain gages were installed on girders G8 and G9 within the second span from the west abutment, shown in Figure 9. The gages were installed on the thinner of the two lower flange plates within 6" (horizontally) of the groove welds. Two gages per girder were used, one near each lower flange splice at approximately the third points. This is shown in Figure 10.

Strain gage data was recorded for 239 truck events. The strain gage monitoring system was configured to record data from all four gages when gage 1 reached +/- 400 PSI. This eliminated data corresponding only to cars and light trucks. Data was stored from 1.5 seconds before to 1.5 seconds after each truck event, to ensure that the peak portion of the loading range was captured. The recording speed was 30 readings per second per gage. Figure 11 and 12 show typical stress versus time plots for a truck event.

The effective stress ranges at each gage location were determined. The resulting histograms are shown in Figures 13 through 16 for each of the four gages.

The estimation of the fatigue resistance was based on Fisher's recommendations in his report (4). These recommendations are based on crack propagation expressions developed from a fracture mechanics analysis of the weld defects.

According to Fisher, the cracks would be susceptible to growth if:

$$\Delta K \geq \Delta K_{TH}$$

where:

$$\Delta K = S_r \sqrt{\pi a}$$

- a = half length of central through-thickness crack
- ΔK = stress intensity range
- ΔK_{TH} = crack growth threshold (the value of 2.75 KSI assumes a high tensile residual stress at the weld)

Fisher's report indicates that the maximum observed crack length was 0.5 inches, equal to twice a . This yields:

$$\Delta K = S_r \sqrt{\pi (0.25)} = 0.886 S_r$$

Solving Equation 2 for S_r , shows that S_r must equal or exceed 3.1 KSI for the cracks to propagate. The maximum calculated effective stress range of 1.65 KSI is well below 3.1 KSI.

Based on the effective stress ranges at typical weld locations, future crack propagation is unlikely. Thus, remedial action is not required and it is not necessary to make expensive repairs. Although no crack propagation was observed, or is likely to occur in the future, the normal biannual field inspections should continue for the life of the superstructure.

Chapter 6

ROUTE 8 BRIDGE IN TRUMBULL

This study was performed to estimate the live load rating. Analytical calculations indicated that the live load capacity was not adequate for the present use. Strain gage testing was used to provide a more accurate assessment of the actual capacity.

This bridge carries 3 lanes of traffic in one direction. The plan is shown in Figure 17. The superstructure consists of simple span welded steel plate girders supporting a concrete deck. The 7 longitudinal girders are composite with the concrete deck. An adjacent, identical, structure carries southbound traffic. Only the structure carrying northbound traffic was tested. The structure is approximately 25 years old and carries low to moderate truck traffic.

At midspan, the center girder and the exterior girders have smaller plates than the rest of the girders. Girders 1 (exterior), 4 (center) and 7 (exterior) use 16" x 2" lower flange plates at midspan while the rest of the girders use 18" x 2"

plates.

Using current code provisions, the center girder has a design live load capacity rating of HS-9.9. Thus, the code based analysis concludes that structure has just under fifty percent of the required live load capacity. Hence, the analysis indicates that the structure is inadequate and that the planned asphalt overlay of the deck should be avoided until the structure is strengthened.

Strain gages were installed on girders 4 and 5 near the midspan of the girders, shown in Figure 18. The gages were installed on the top face of the lower flange plates.

Strain gage data was recorded for 62 truck events. The strain gage monitoring system was configured to record data from both gages when either gage reached a live load stress of +500 PSI. This eliminated data corresponding only to cars and light trucks. Data was recorded from 1.5 seconds before to 1.5 seconds after each truck event. The recording speed was 30 readings per second per gage.

Figures 19 and 20 show the maximum observed stresses for the two strain gages, equal to 1.60 KSI and 2.15 KSI for two typical data sets. The center girder experienced the greater stress levels of the two girders in 25 of the 62 recorded truck events. Thus, it is likely that the larger stress has more to do with the truck's position on the deck than the plate size difference between the two girders. Visual observation of trucks passing the bridge confirmed this. The weaker girder does not always experience greater stress levels. In fact the weaker girders reduced stiffness probably allows more load to be transferred to the adjacent girders. The heaviest observed truck was a loaded tractor trailer. It is clear that the actual live load stresses are considerably smaller than the computed stresses based upon AASHTO assumptions.

The bridge was reanalyzed using the maximum live load data obtained from the field strain monitoring. The maximum observed stresses were doubled to account for the possibility of simultaneous multiple truck loading. The resulting live load rating was in excess of HS-30, exceeding the required live load capacity of HS-20 by more than 50 percent. Hence, no strengthening of the bridge girders was required, with a saving

in both time and expense. The deck overlay and joint repairs could continue as planned.

Chapter 7

Conclusions

This report demonstrates the benefits of using field strain gage testing to generate information on the actual behavior of different steel bridges. Analyses do not always adequately predict stress level, particularly in localized areas of connection elements and members. This is often due to difficulties in accounting for stress concentrations. At other times redundancy makes analytical predictions approximate at best. Field testing, combined with careful analyses, can provide many answers where analyses are approximate at best.

This report presents four case studies which were used to determine whether changes and/or repairs were necessary. The results of these case studies are:

- (1) The stresses in the corroded hangers for a 70 year old drawbridge were high. Thus emergency repairs were needed, even though the bridge was scheduled for replacement.

(2) The cause of cracking in the vicinity of the diaphragm connections in a 15 year old steel girder bridge was not a result of excessive stresses. Instead it was due to poor welds made during fabrication. The conclusion of the study was that repairs were not needed.

(3) The effective stress range in a 35 year old interstate bridge subject to heavy truck traffic was low enough so that fatigue should not be a problem. Thus repairs, which would be costly, were not needed.

(4) The load rating in a 25 year old bridge, due to varying girder sizes across the bridge width, was predicted by analyses to be half the required load rating. Testing demonstrated that the smaller girders do not receive as much live load as predicted by the analyses and thus are not overstressed. Therefore, it was concluded that it is not necessary to carry out strengthening, saving both time and expense.

REFERENCES

1. Sartor, R.R., "Strain Monitoring of Highway Bridge Structures," thesis presented to University of Connecticut in partial fulfillment of the requirements for the Degree of Master of Science, Storrs, CT, 1995.
2. DeWolf, J.T. and Bernard, K.J., "Fatigue Failure Investigation - Putnam Bridge," Civil Engineering Department Report JHR 94-237, University of Connecticut, Storrs, CT, 1994.
3. "Guide Specification for Fatigue Evaluations of Existing Steel Bridges," The American Association of State Highway and Transportation Officials, Washington, D.C., 1990 and 1993 revision.
4. Fisher, J.W., Report to Mr. Steven M. Barton of the Connecticut Department of Transportation, RE: Yankee Doodle Bridge, April 1993.

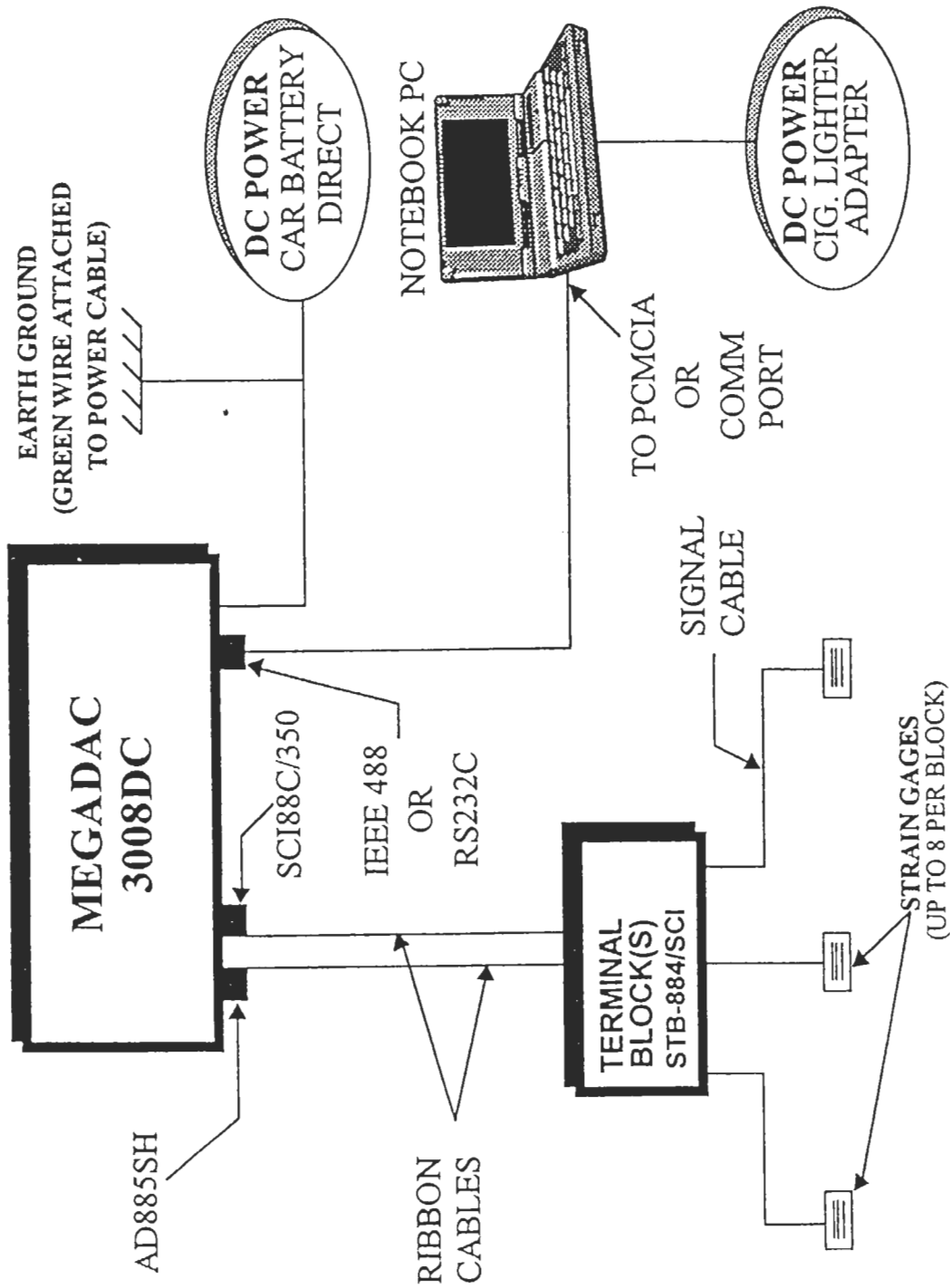


Figure 1: Strain Gage Monitoring System

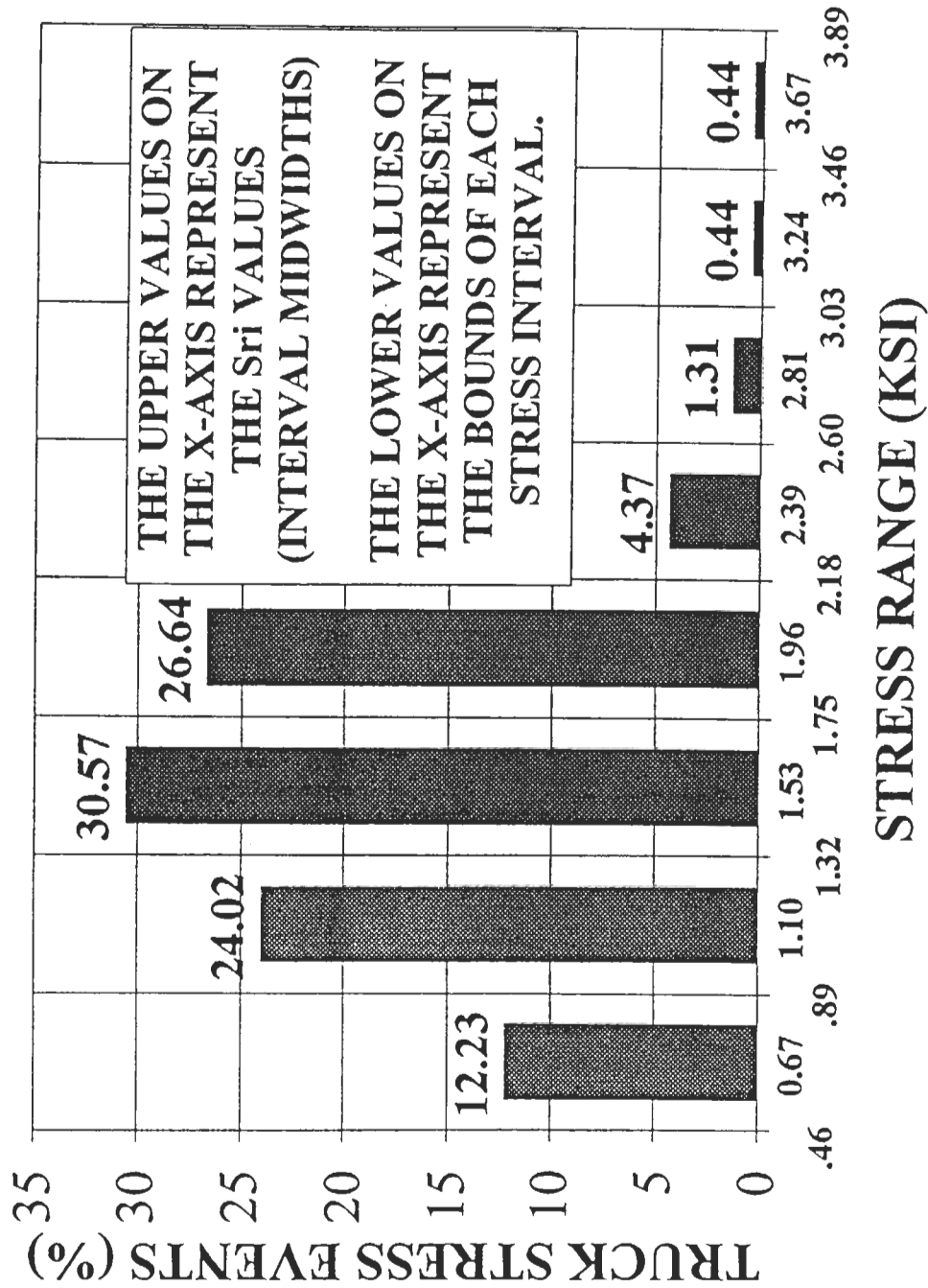


Figure 2: Stress Range Histogram

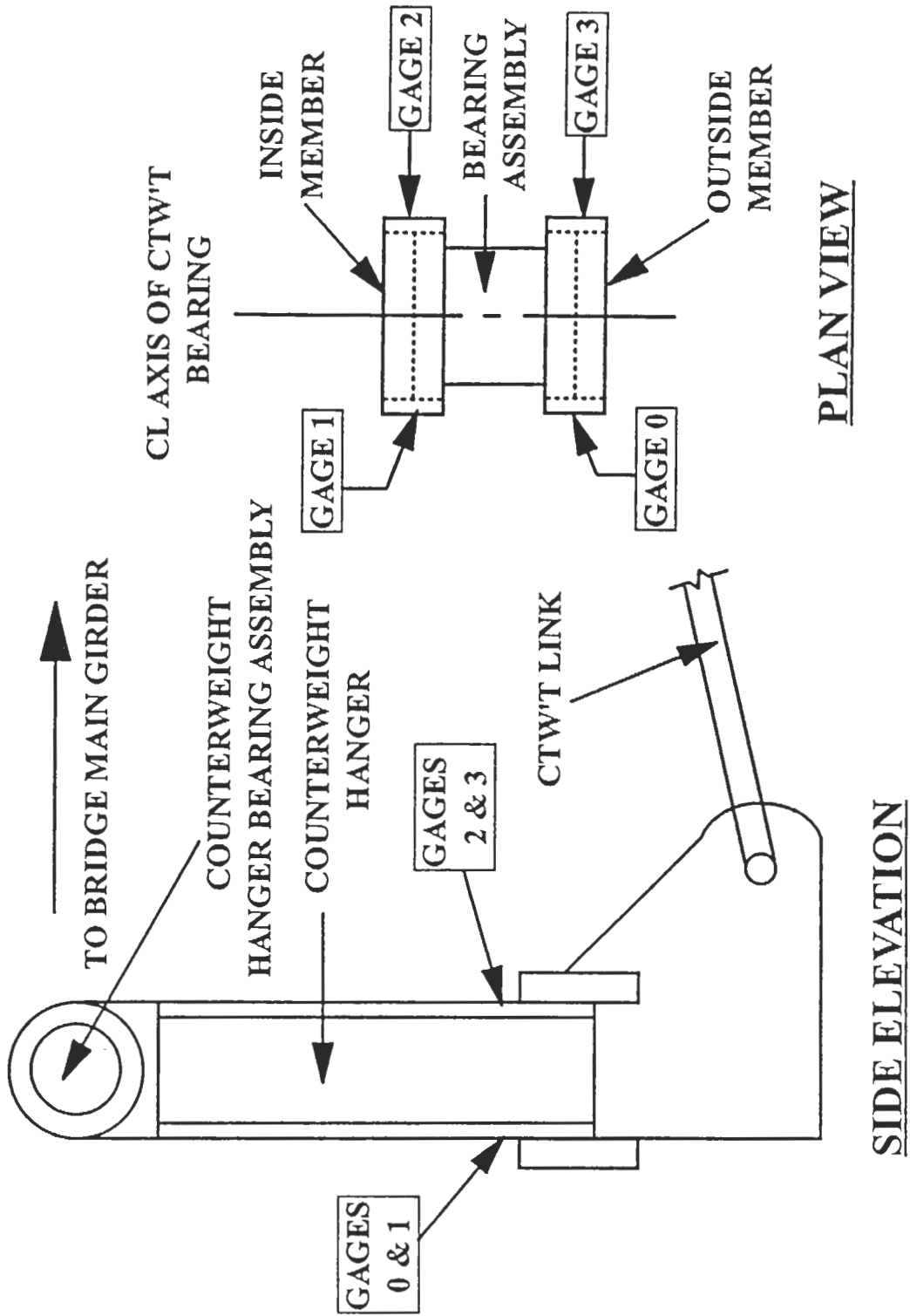


Figure 3: Tomlinson Bridge Hanger Assembly

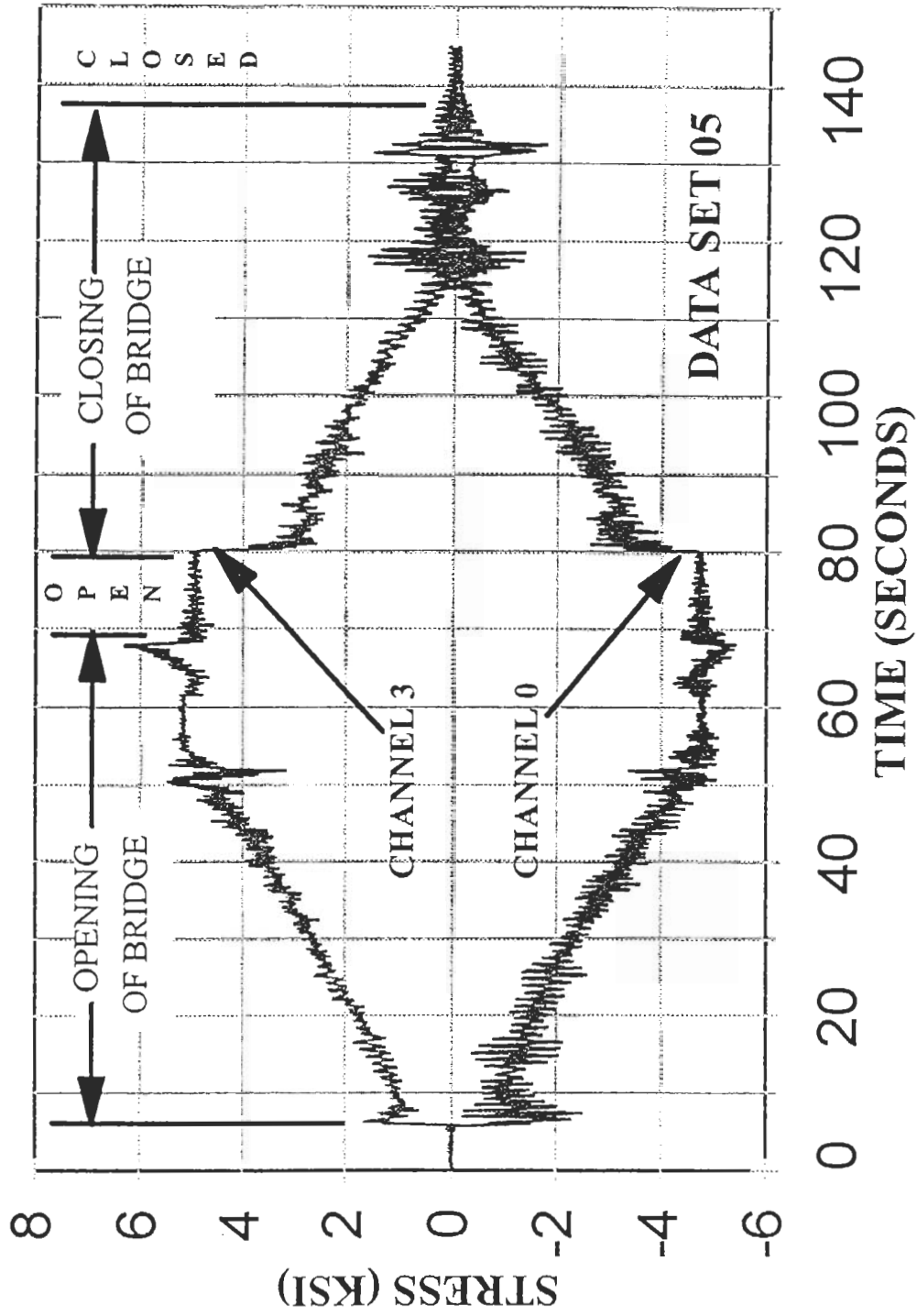


Figure 4: Tomlinson Bridge - Stress VS. Time (Outside Hanger Member)

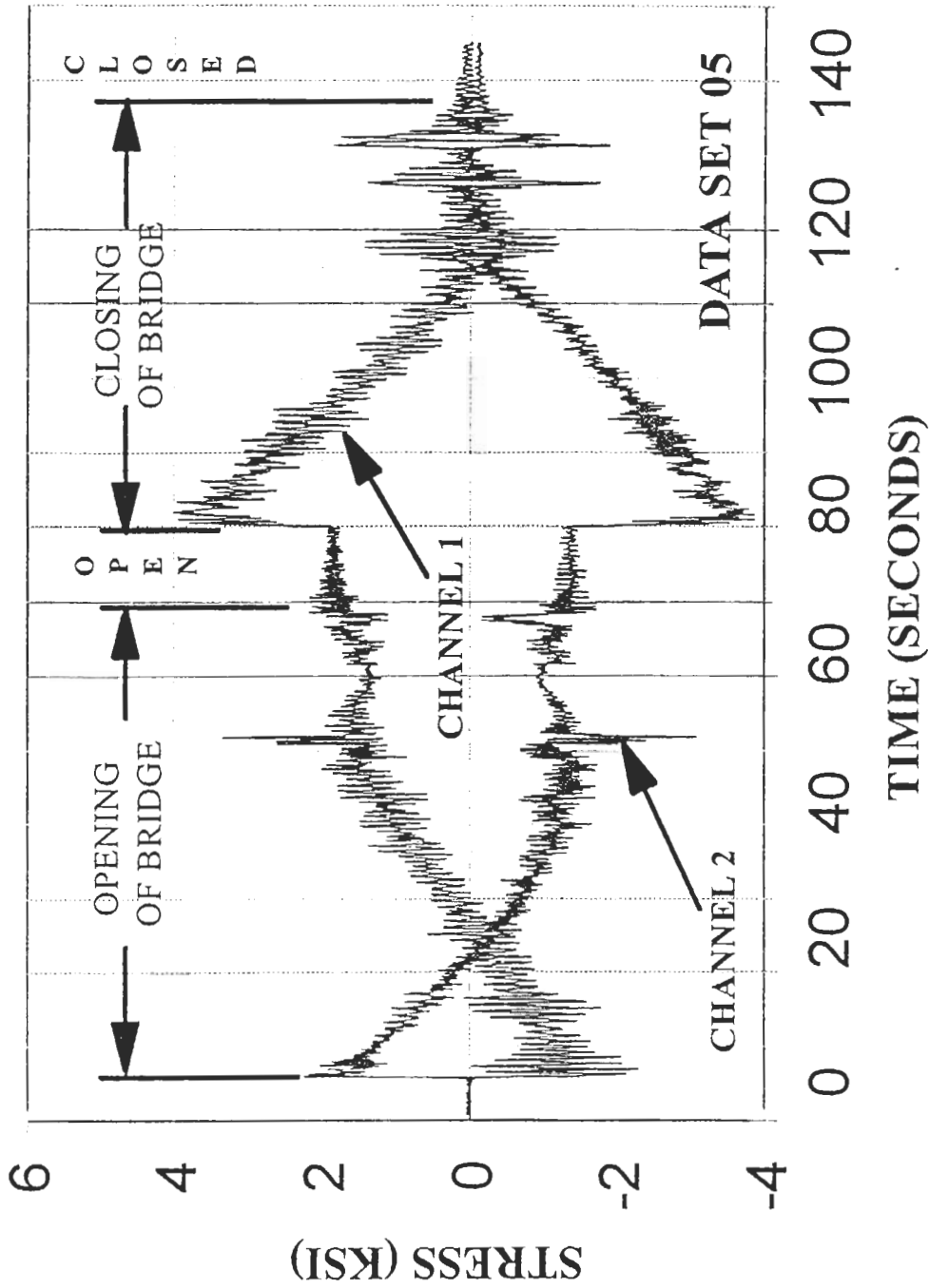


Figure 5: Tomlinson Bridge - Stress VS. Time (Inside Hanger Member)

FIGURE 5.1: STRAIN GAGE LOCATIONS

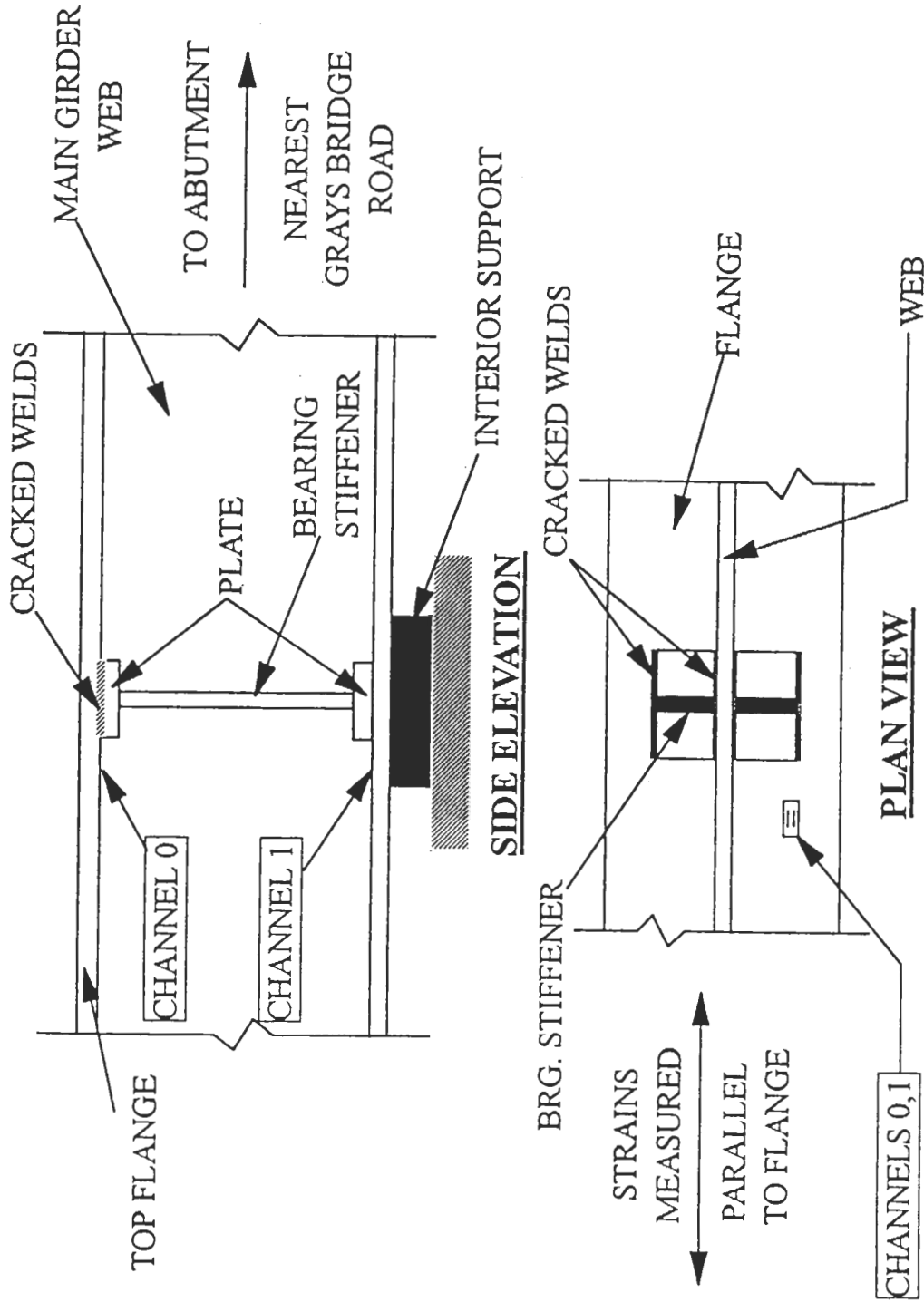


Figure 6: Route 7 Bridge - Cracking And Strain Gage Locations

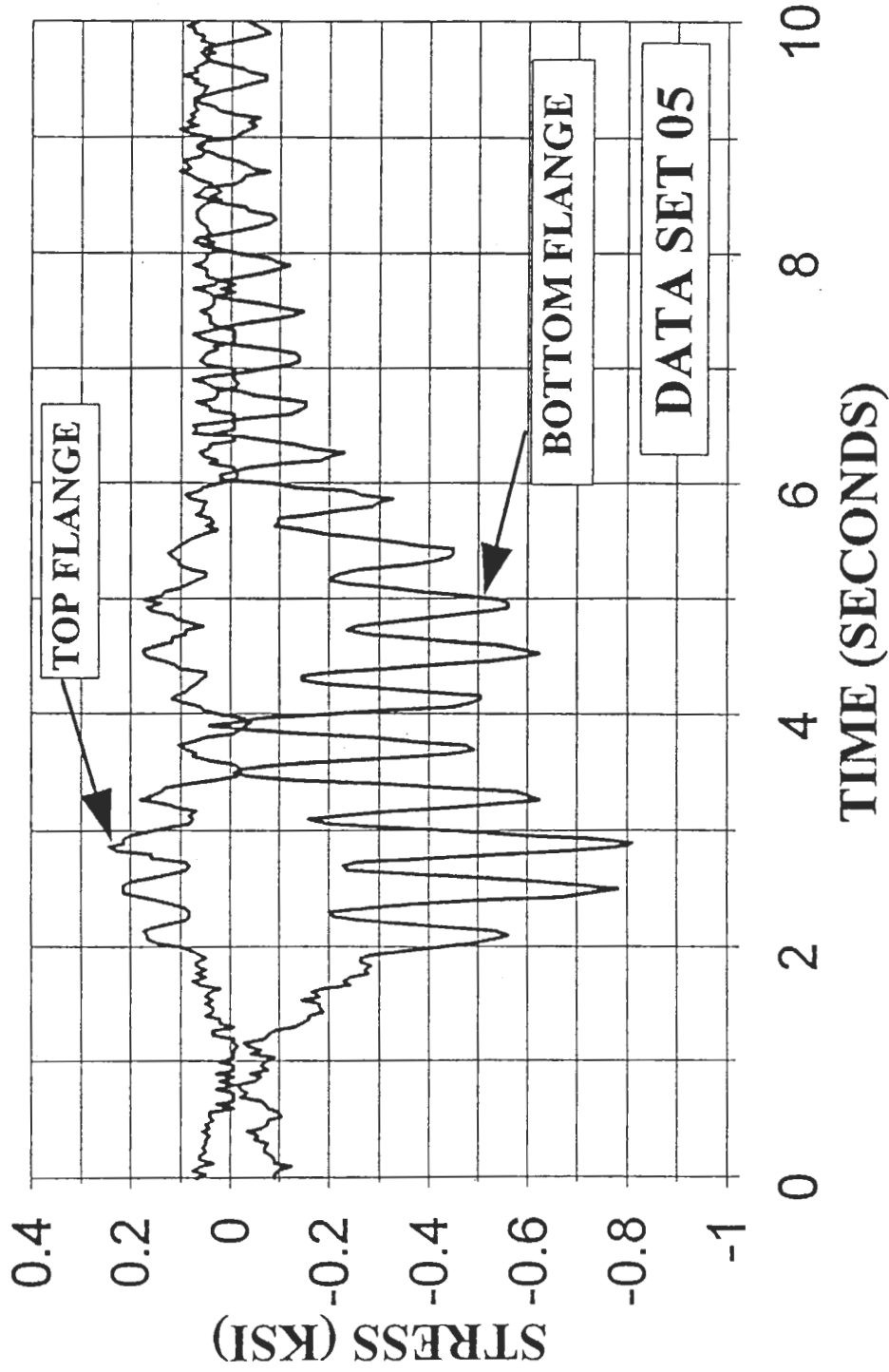


Figure 7: Route 7 Bridge - Typical Plot of Stress vs. Time

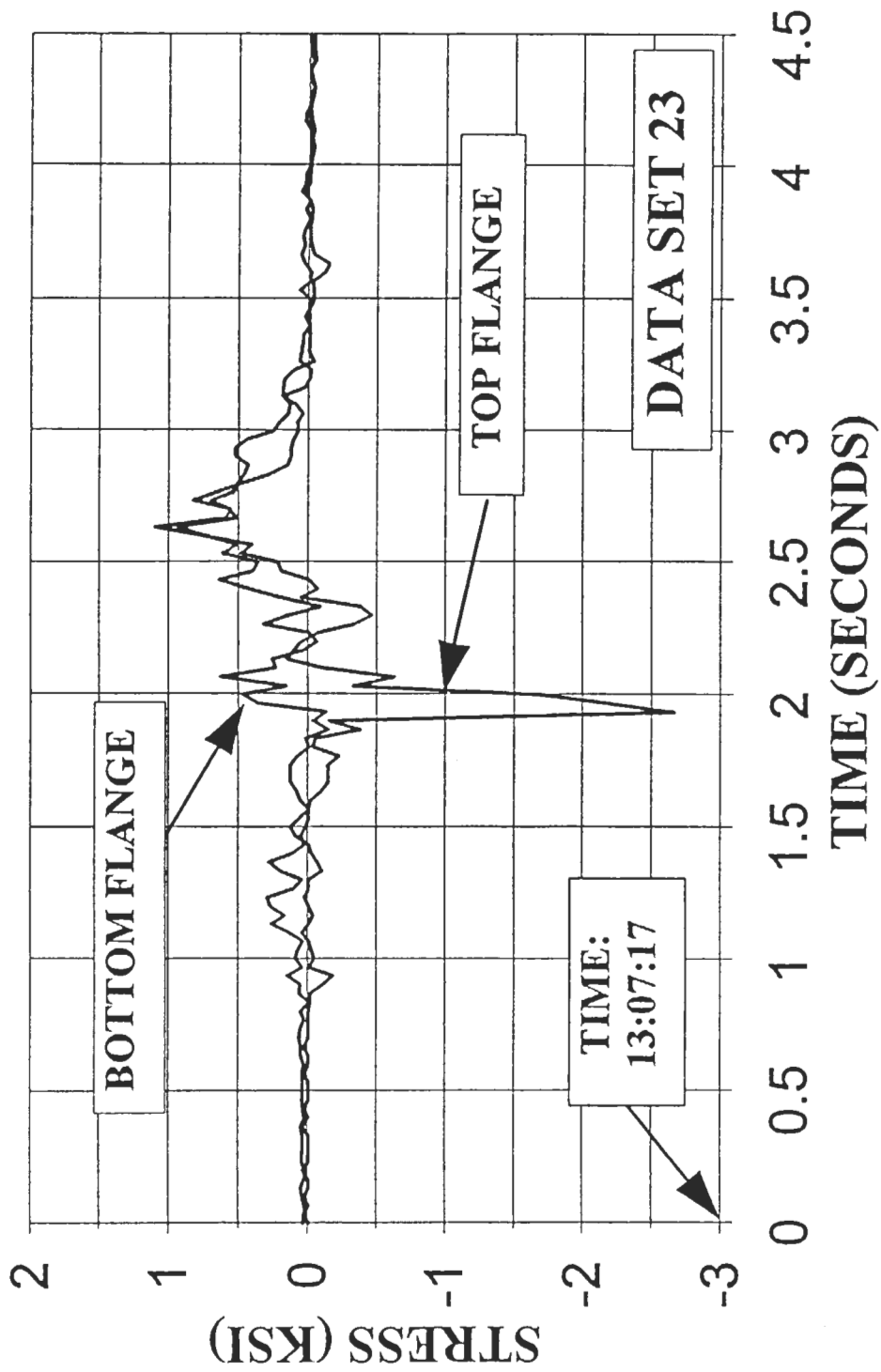


Figure 8: Route 7 Bridge - Non-Typical Plot of Stress vs. Time

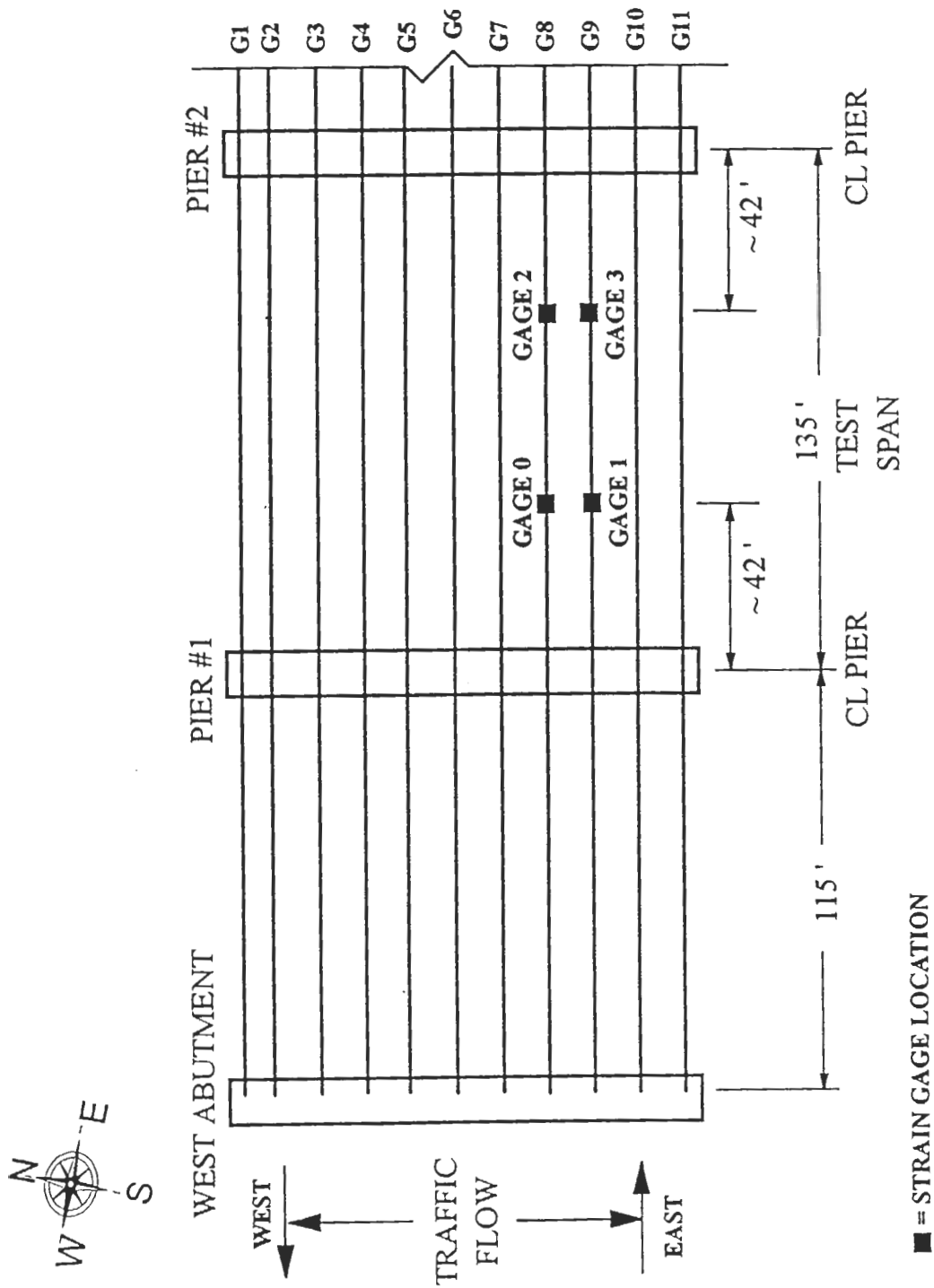


Figure 9: Yankee Doodle Bridge - Plan View Of Test Span With Strain Gage Locations

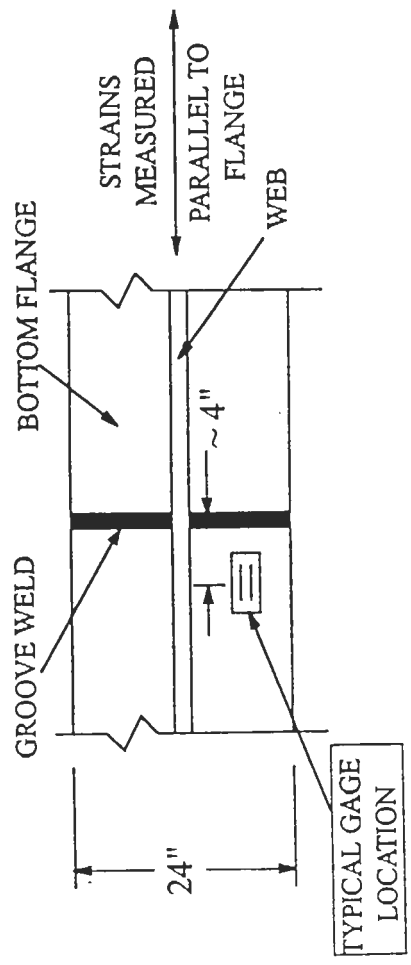
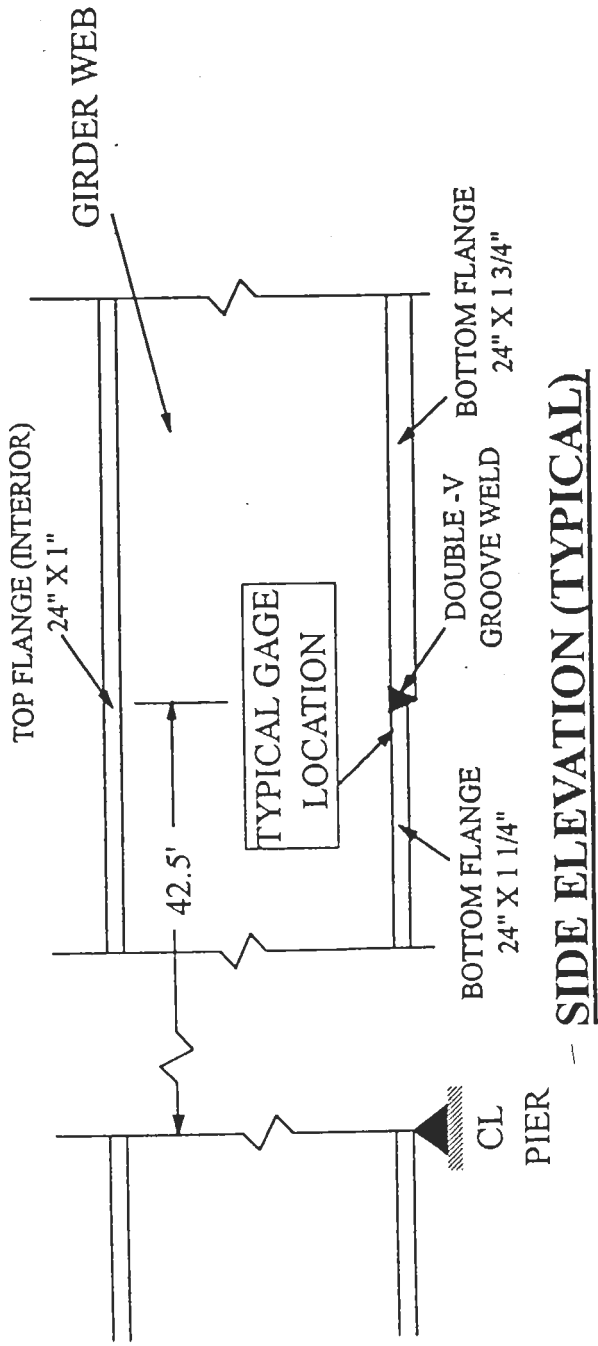


Figure 10: Yankee Doodle Bridge - Detail With Strain Gage Location

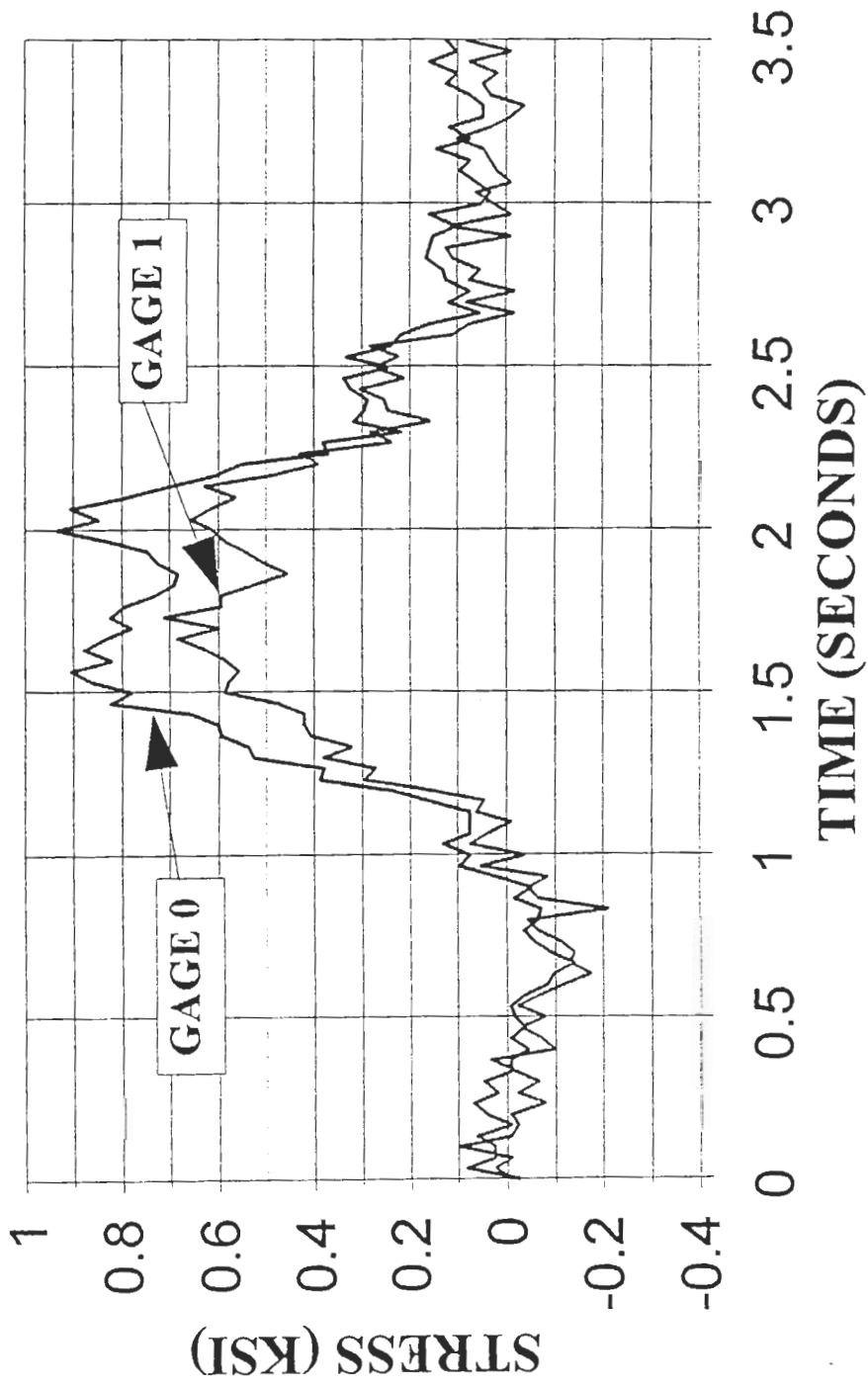


Figure 11: Yankee Doodle Bridge-Typical Plot Of Stress VS. Time

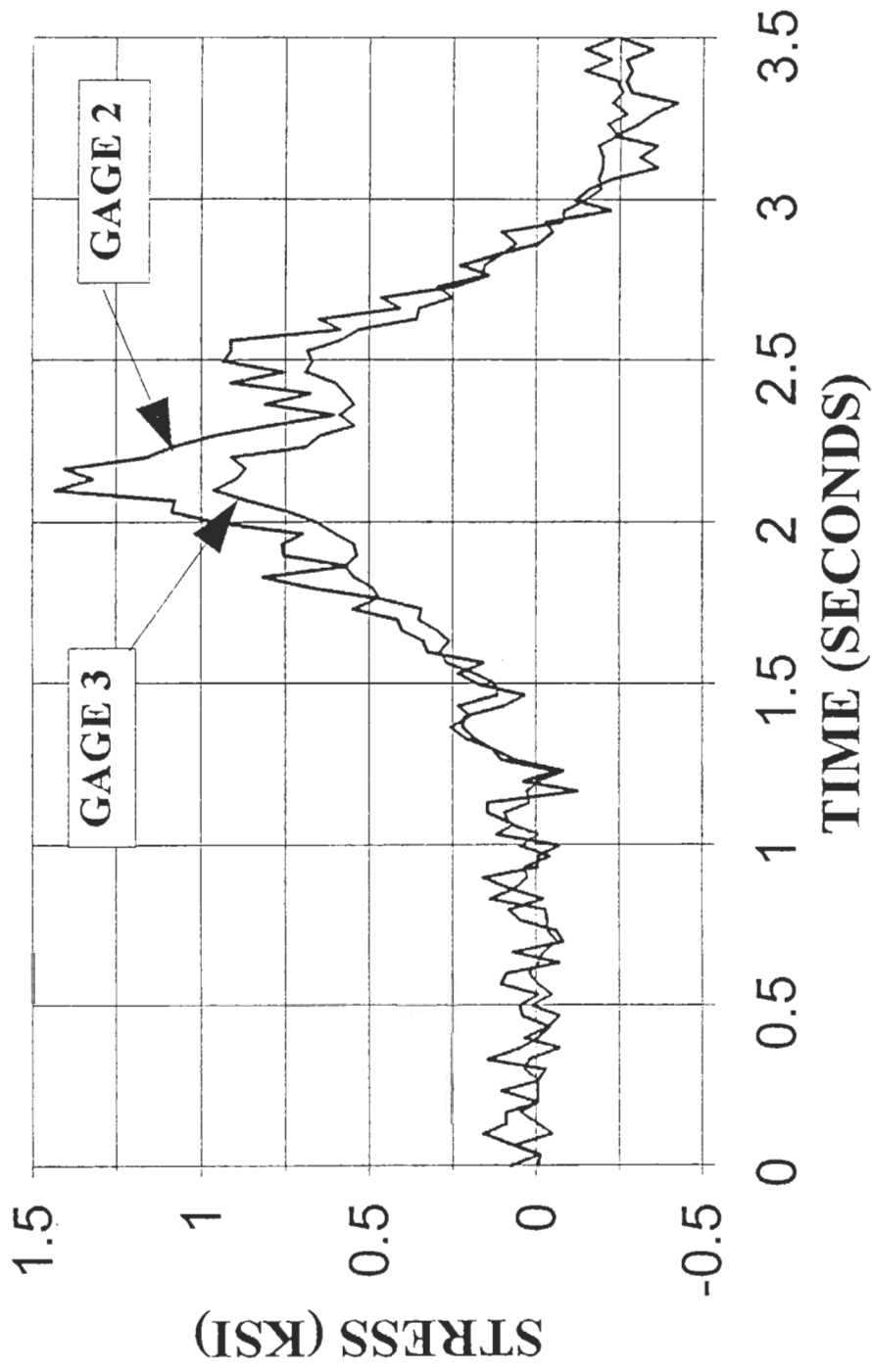


Figure 12: Yankee Doodle Bridge - Typical Plot Of Stress VS. Time

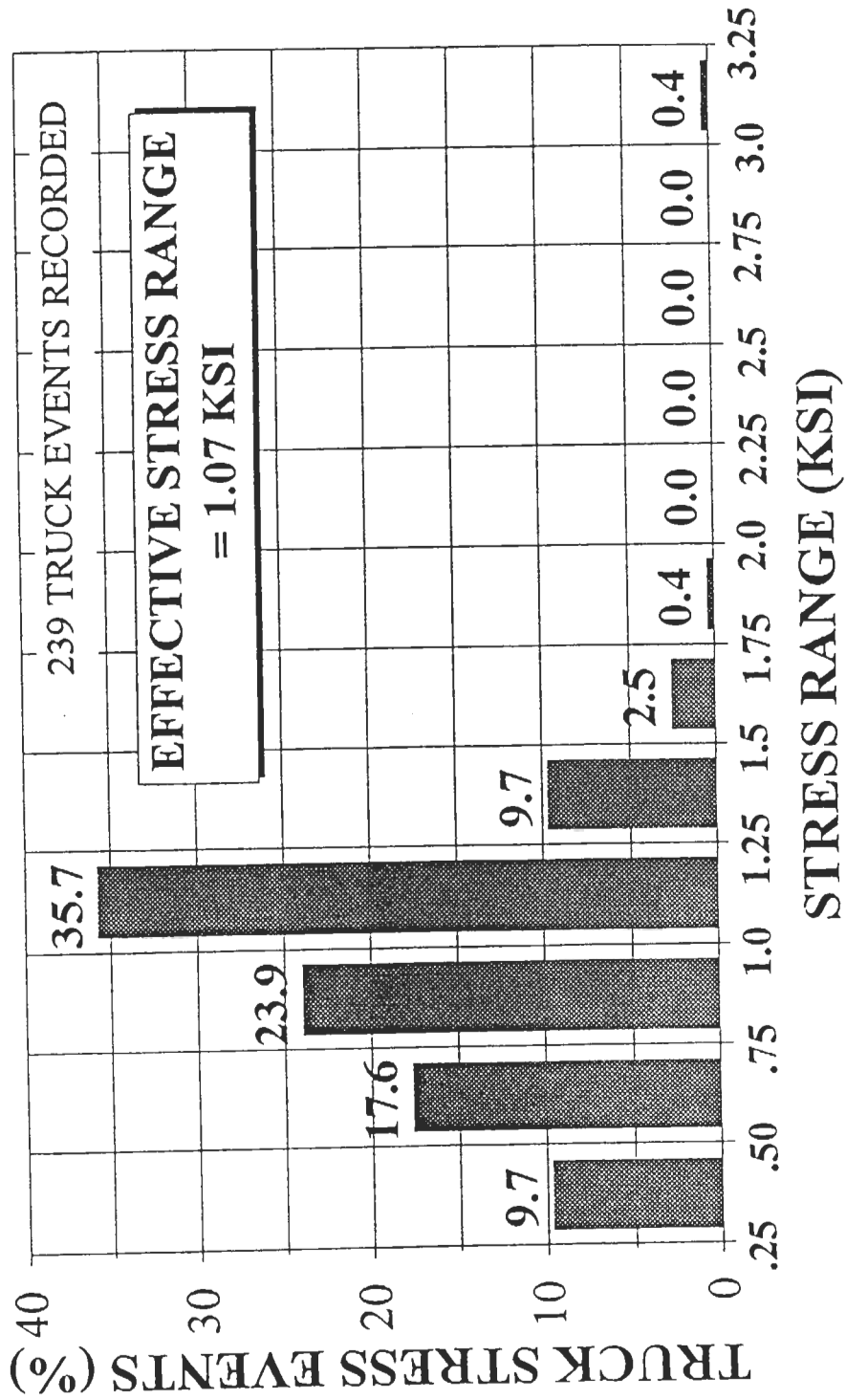


Figure 13: Yankee Doodle Bridge - Stress Range Histogram For Channel 0

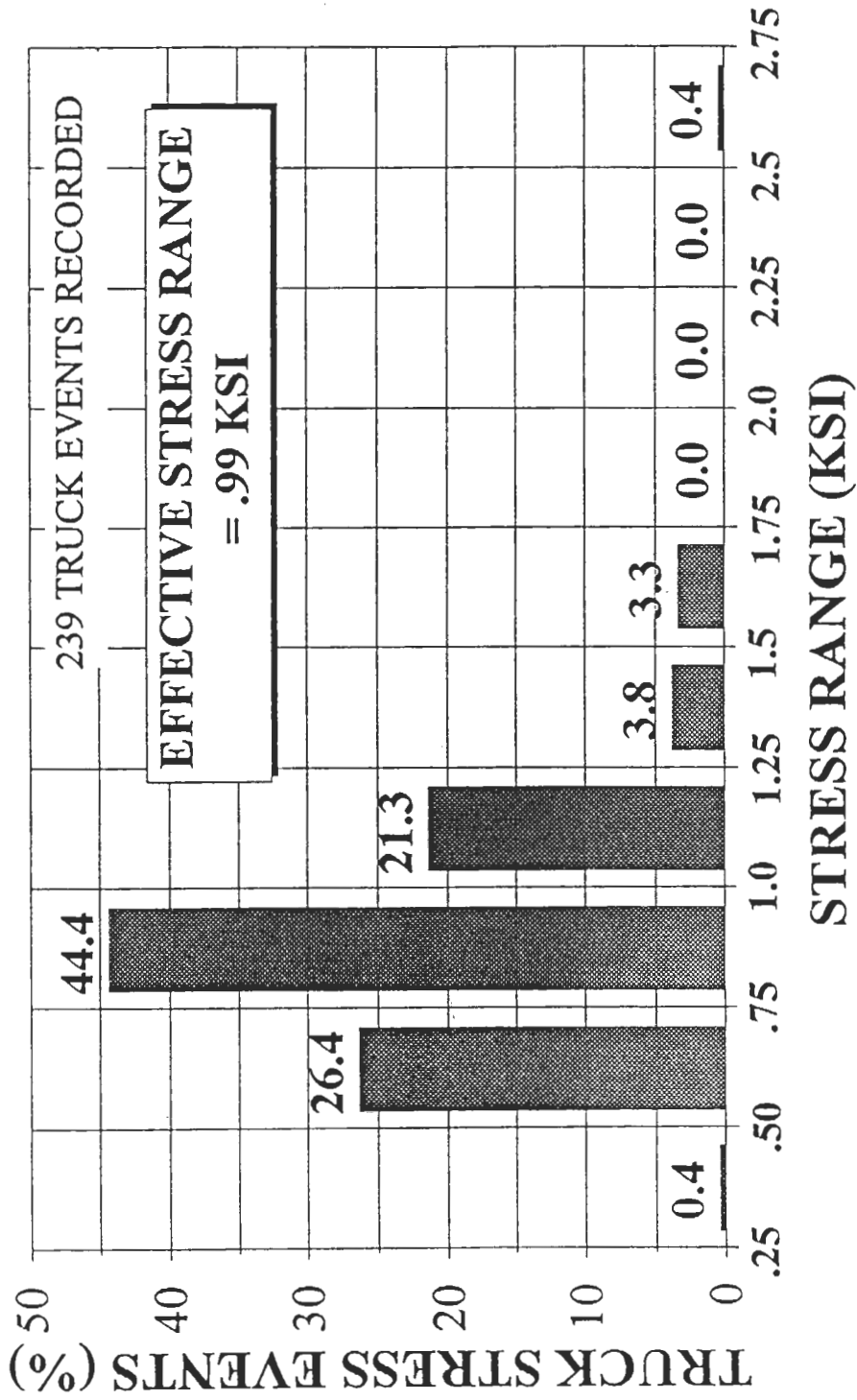


Figure 14: Yankee Doodle Bridge - Stress Range Histogram For Channel 1

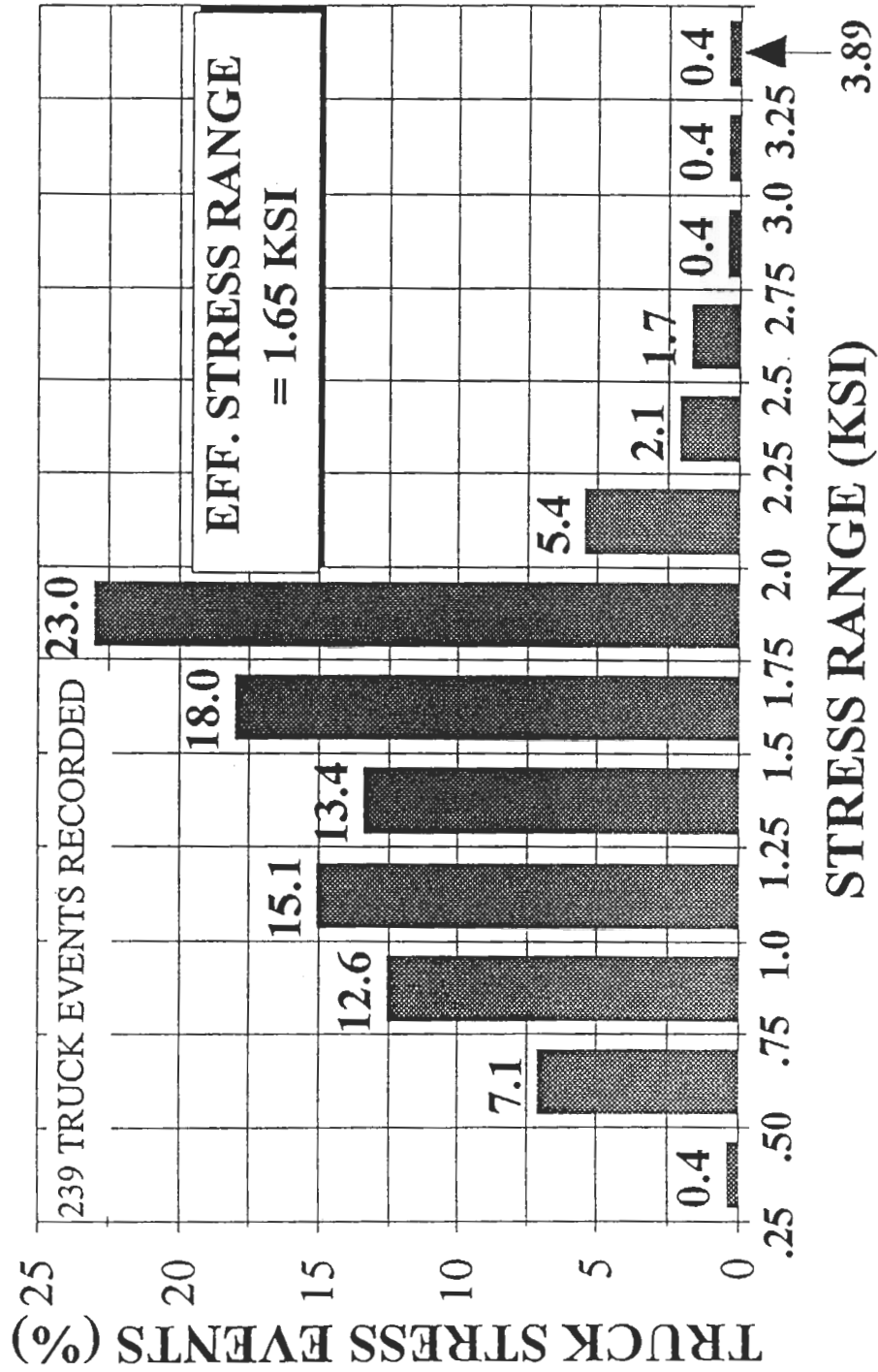


Figure 15: Yankee Doodle Bridge - Stress Range Histogram For Channel 2

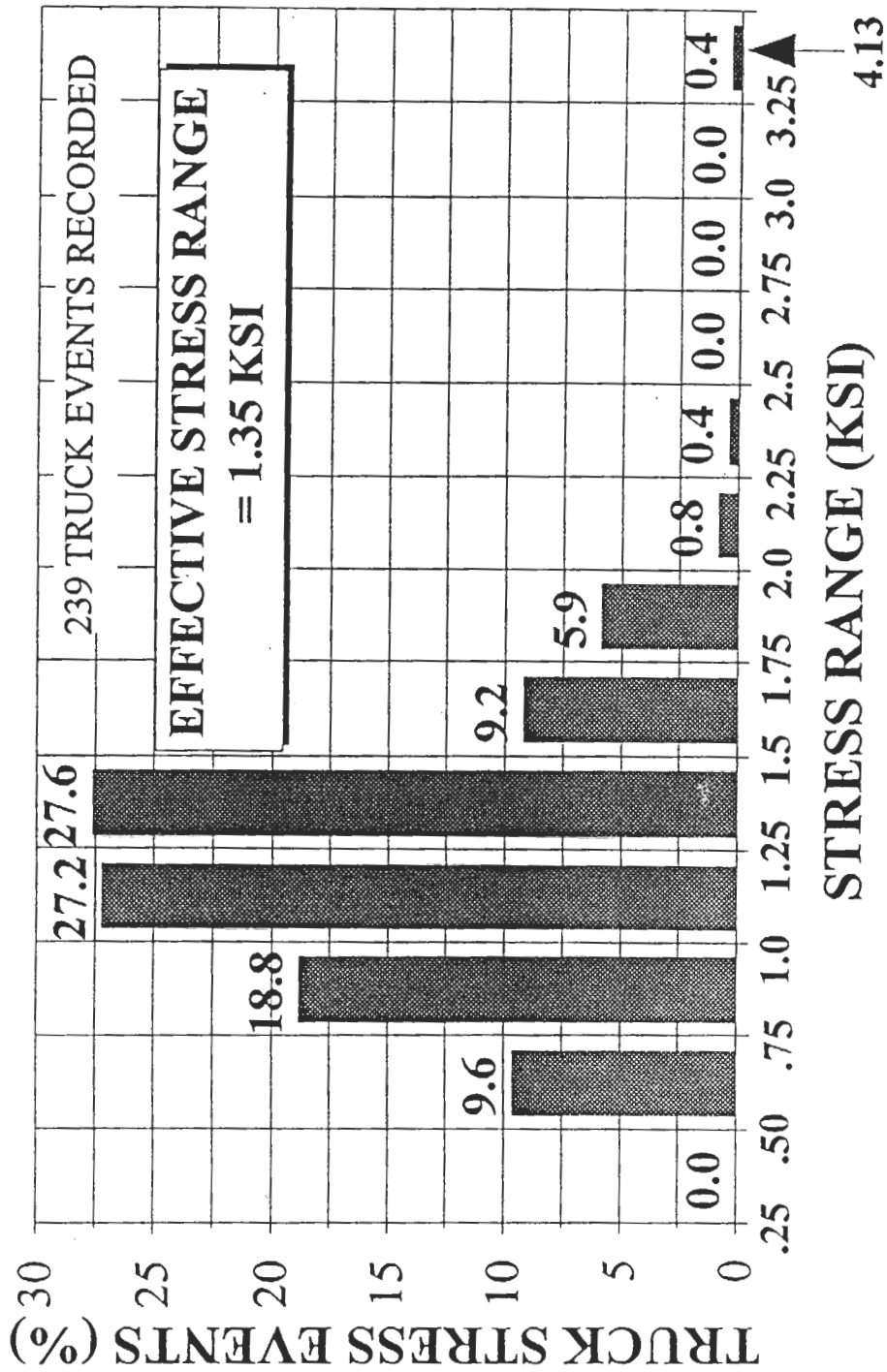


Figure 16: Yankee Doodle Bridge - Stress Range Histogram For Channel 3

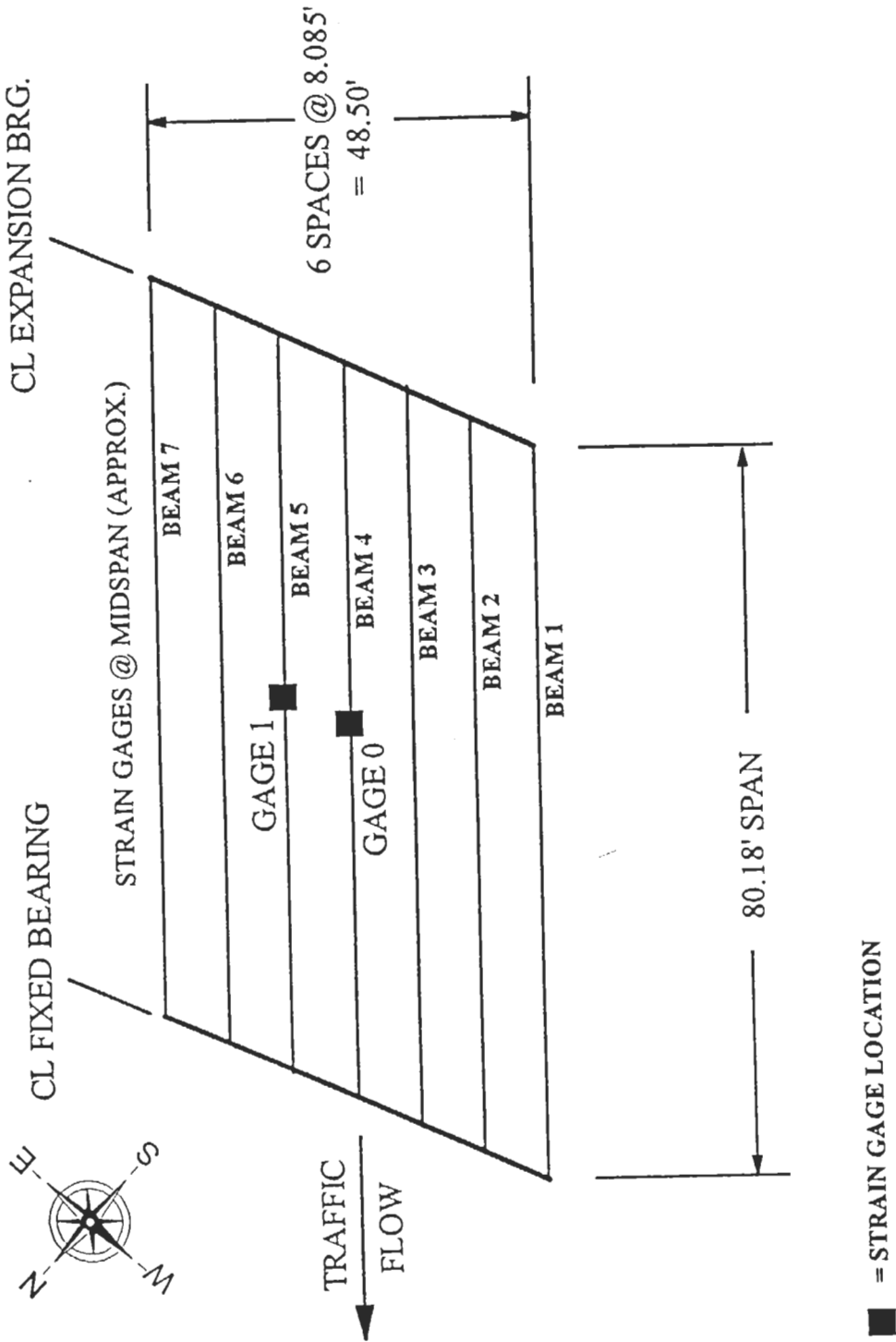


Figure 17: Route 8 Bridge - Plan View With Strain Gage Locations

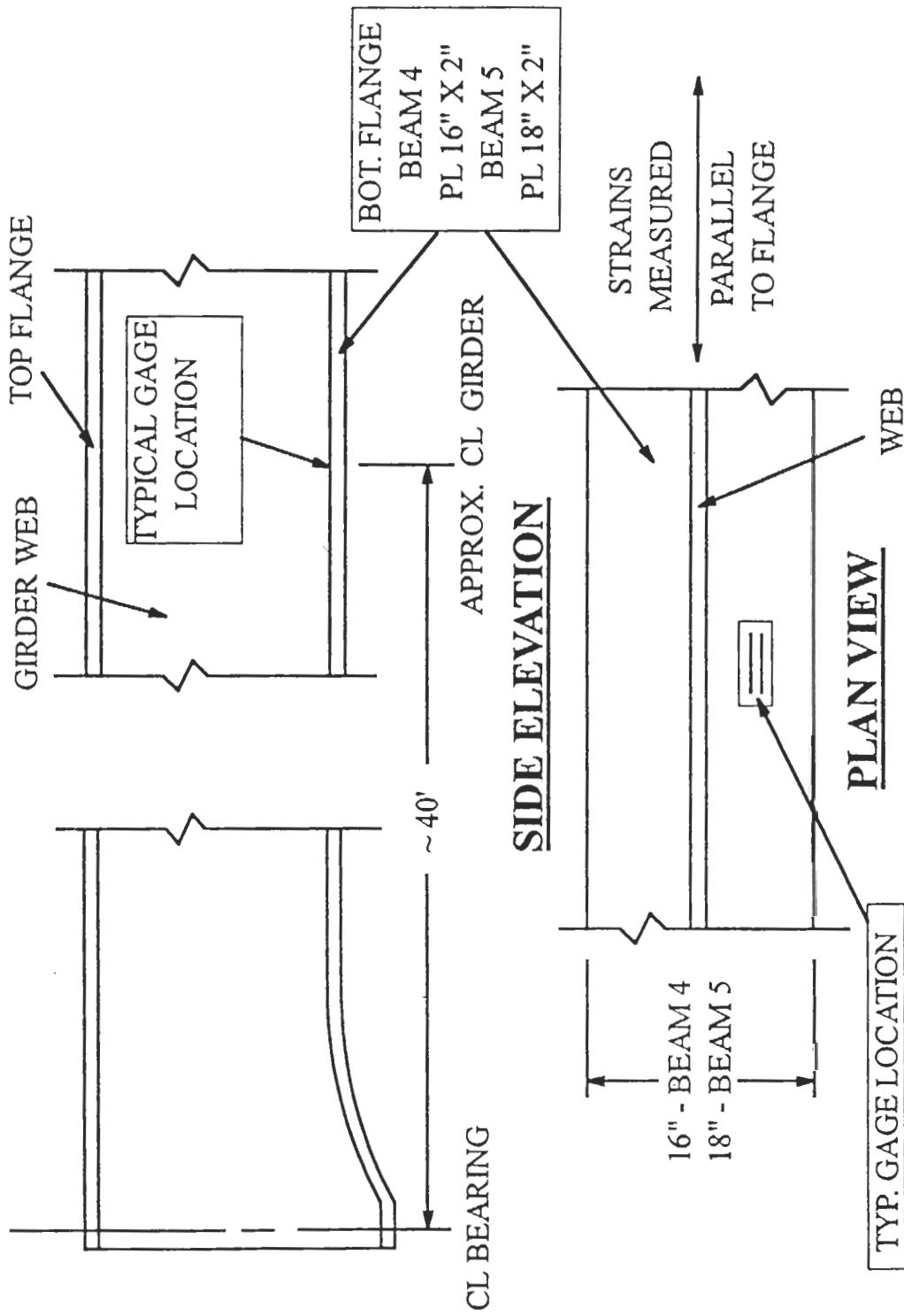


Figure 18: Route 8 Bridge - Detail With Strain Gage Location

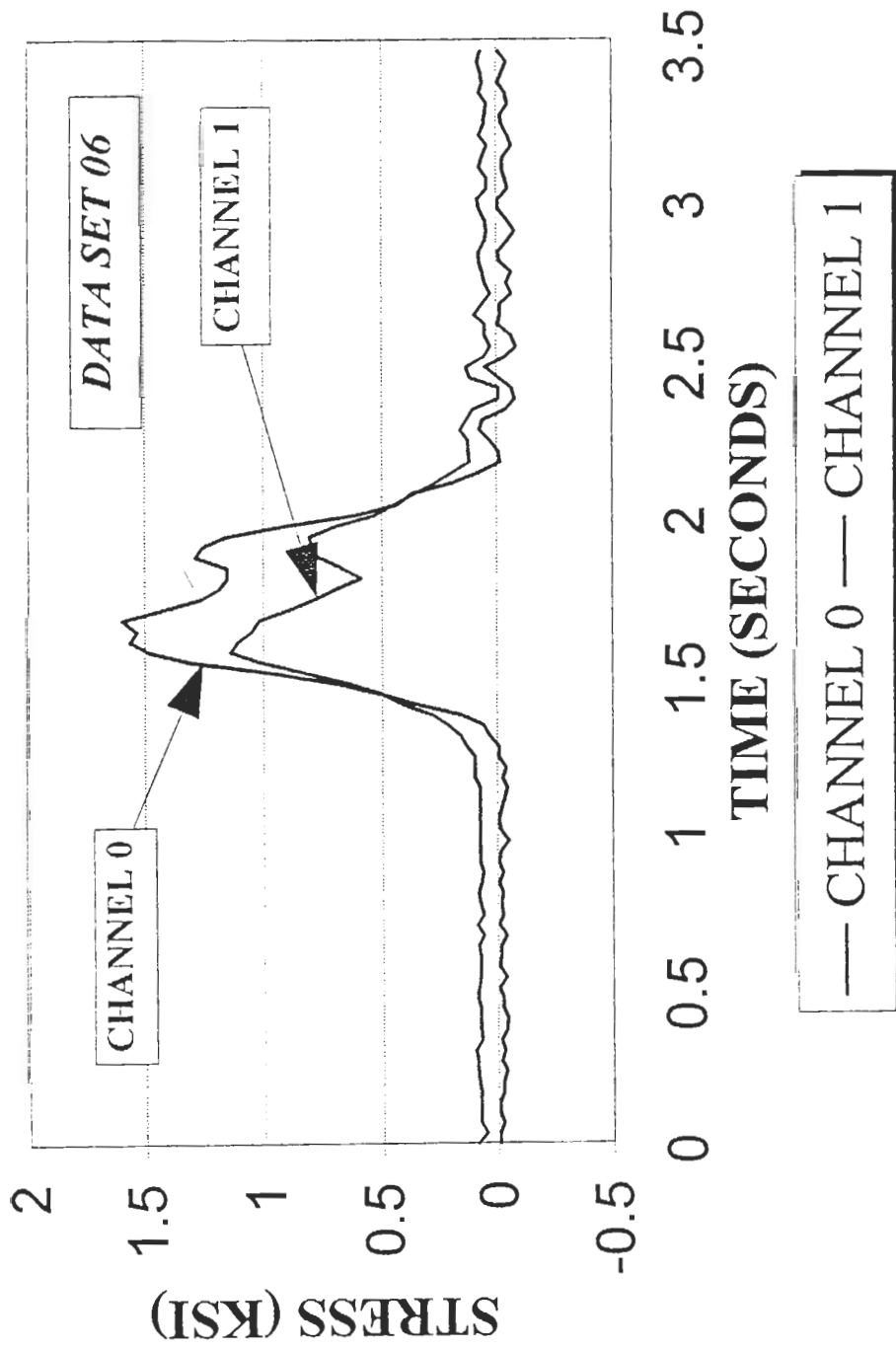


Figure 19: Route 8 Bridge Plot of Stress vs. Time Data Set 06

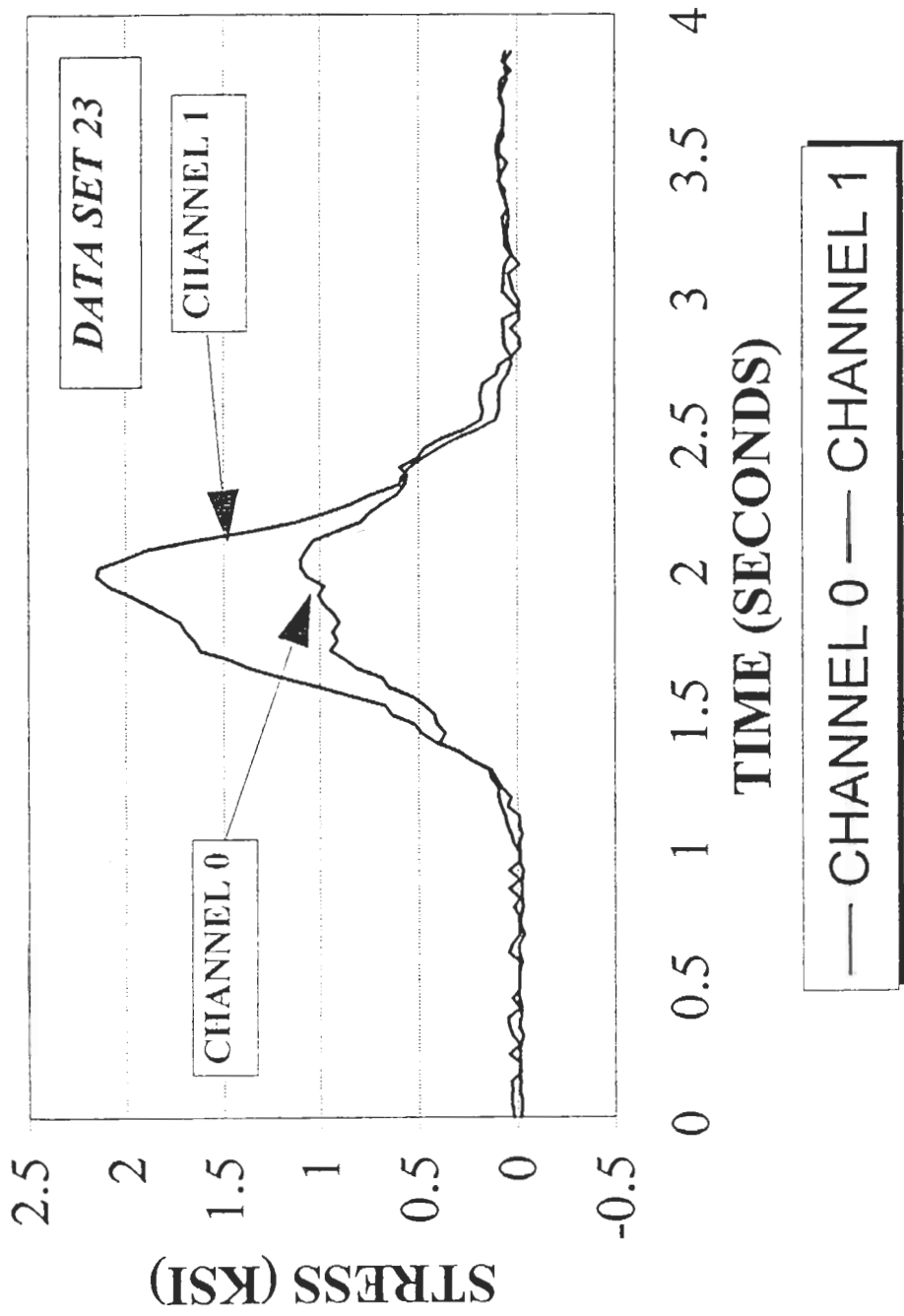


Figure 20: Route 8 Bridge Plot Of Stress VS. Time Data Set 23

TABLE 1: Tomlinson Bridge - Maximum Stress Levels (KSI)

DATA SET	CHAN 0 outside	CHAN 1 inside	CHAN 2 inside	CHAN 3 outside	DESCRIPTION OF DATA SET
1	-5.6	2.9	-2.8	6.4	OPENING OF BRIDGE (DATA SETS 1 & 2 FORM 1 CYCLE)
2	-4.5	4.2	-4.1	4.3	CLOSING OF BRIDGE
3	-5.3	3.5	-3.2	6.1	OPENING OF BRIDGE (DATA SETS 3 & 4 FORM 1 CYCLE)
4	-4.4	4.4	-4.2	4.8	CLOSING OF BRIDGE
5	-5.4	4.0	-3.9	6.3	COMPLETE CYCLE (OPENING AND CLOSING)
6	-5.6	3.9	-3.7	6.6	COMPLETE CYCLE (OPENING AND CLOSING)

TABLE 2: Route 7 Bridge - Maximum Streeses (KSI)

TEST NAME	DATA SET	MAXIMUM STRESS PER DATA SET	
		TOP FLANGE (CHANNEL 0) TENSION	BOTTOM FLANGE (CHAN. 1) COMPRESSION
BROOK1	1	.104	.456
	2	.187	.546
	3	.124	.45
	4	.207	.789
	5	.242	.809
BROOK2	6	.214	.6638
	7	.18	.581
	8	.1305	.560
	9	.0899	.249
	10	.242	.858
BROOK3	11	.076	.367
	12	.097	.491
	13	.263	.712
BROOK4	14	.152	.519
	15	.194	.692
	16	.242	.851
	17	.235	.74
	18	.131	.532
	19	.131	.422
	20	.200	.712
	21	.263	.823
	22	.041	.408
	23	1.09; -2.66	-.145; +.93
	24	.187	.657
	25	.021	.367
AVERAGE STRESS		.165 KSI	.594 KSI